

Tougher ultrafine grain Cu via high-angle grain boundaries and low dislocation density

Y. H. Zhao,^{1,6,a)} J. F. Bingert,¹ Y. T. Zhu,^{1,b)} X. Z. Liao,² R. Z. Valiev,³ Z. Horita,⁴ T. G. Langdon,⁵ Y. Z. Zhou,⁶ and E. J. Lavernia⁶

¹Los Alamos National Laboratory, Los Alamos, New Mexico 87545, USA

²School of Aerospace, Mechanical and Mechatronics Engineering, The University of Sydney, Sydney, New South Wales 2006, Australia

³Institute of Physics of Advanced Materials, Ufa State Aviation Technical University, Ufa 450000, Russia

⁴Department of Materials Science and Engineering, Kyushu University, Fukuoka 819-0395, Japan

⁵Departments of Aerospace and Mechanical Engineering and Materials Science, University of Southern California, Los Angeles, California 90089-1453, USA

⁶Department of Chemical Engineering and Materials Science, University of California, Davis, California 95616, USA

(Received 25 November 2007; accepted 25 January 2008; published online 25 February 2008)

Although there are a few isolated examples of excellent strength and ductility in single-phase metals with ultrafine grained (UFG) structures, the precise role of different microstructural features responsible for these results is not fully understood. Here, we demonstrate that a large fraction of high-angle grain boundaries and a low dislocation density may significantly improve the toughness and uniform elongation of UFG Cu by increasing its strain-hardening rate without any concomitant sacrifice in its yield strength. Our study provides a strategy for synthesizing tough UFG materials. © 2008 American Institute of Physics. [DOI: 10.1063/1.2870014]

Bulk nanostructured (NS) and ultrafine grained (UFG) materials usually have high strength but disappointingly low ductility.¹ It is now well established that the low ductility of NS and UFG materials is caused by either extrinsic flaws such as porosity or intrinsic microstructures that possess low strain hardening/dislocation storage capacity. Accordingly, several different strategies have been developed recently to improve the poor ductility of NS materials, including the introduction of a bimodal grain size distribution,² the preexisting nanoscale twins,^{3,4} dispersions of nanoparticles and nanoprecipitates,⁵ a mixture of two or multiple phases,⁶ transformation- and twinning-induced plasticities,⁷ and changing the deformation conditions.⁸ A few examples of excellent strength and ductility in single-phase UFG metals^{9,10} were recently reported, but the structural features responsible for these results are not well understood. In view of these findings, the objective of the present study was twofold: first, to develop a strategy for increasing the ductility/toughness of large bulk UFG Cu, and second, to evaluate the mechanism contributing to high ductility in UFG Cu.

Two pure copper (99.99%) samples were processed by severe plastic deformation (SPD) techniques to form two different UFG structures. The first was a Cu bar processed by equal-channel angular pressing (ECAP) for 12 passes using route B_C to produce a UFG structure with predominantly low-angle grain boundaries (LAGBs) and high dislocation densities (hereafter, designated as the UFG_{ECAP} sample). The other sample was a pure copper disk with a thickness of 0.8 mm and diameter of 10 mm processed by high pressure torsion (HPT) for five revolutions under a pressure of 6 GPa and then it was cold rolled (CR) to a thin ribbon with a thickness of 0.2 mm to produce a UFG structure with predominantly high-angle GBs (HAGBs) and lower dislocation

densities (henceforth, designated as the UFG_{HPT+CR} sample). Both type of samples were cut and polished into tensile-testing specimens with gauge dimensions of $10 \times 1 \times 0.15$ mm³. Uniaxial tensile tests were performed at room temperature with an initial strain rate of 1.7×10^{-4} s⁻¹. The gauge sections of the tensile specimens were examined using x-ray diffraction (XRD) to determine the dislocation and twin densities. Transmission electron microscopy (TEM) specimens were prepared by mechanical grinding and ion milling with liquid nitrogen cooling. Quantitative electron backscatter diffraction (EBSD) scans were performed on electropolished specimens.

The engineering stress-strain curves of the UFG_{ECAP} and UFG_{HPT+CR} samples are compared in Fig. 1(a). It is apparent that both samples have similar 0.2% yield strengths of ~ 420 MPa (marked by open circles) but they exhibit very different uniform elongations and different stress-strain curves. The UFG_{ECAP} Cu sample started necking shortly after yielding, leading to a uniform elongation of only $\sim 1.0\%$ and an elongation to failure of only $\sim 4.5\%$. By contrast, the UFG_{HPT+CR} sample underwent strain hardening, giving a uniform elongation of $\sim 2.2\%$ and a subsequent elongation to failure of $\sim 5.1\%$. Repeating the tests indicated that the error of the uniform elongation is smaller than 0.5%. Moreover, after the onset of necking, the reduction in the strain-hardening rate in the UFG_{HPT+CR} sample was significantly slower than in the UFG_{ECAP} sample giving a higher toughness. The uniform elongation was determined using the Considère criterion and the limits of uniform elongation are marked by the symbol “□” on every curve.

Figure 1(b) demonstrates that the UFG_{HPT+CR} sample has a higher normalized strain-hardening rate Θ than UFG_{ECAP} Cu and this is consistent with the higher uniform elongation in UFG_{HPT+CR} copper. Specifically, the UFG_{HPT+CR} sample displays a positive strain-hardening rate to a significant strain whereas, by contrast, the rate in the UFG_{ECAP} sample de-

^{a)}Electronic mail: yzhao@ucdavis.edu.

^{b)}Electronic mail: ytzhu@ncsu.edu.

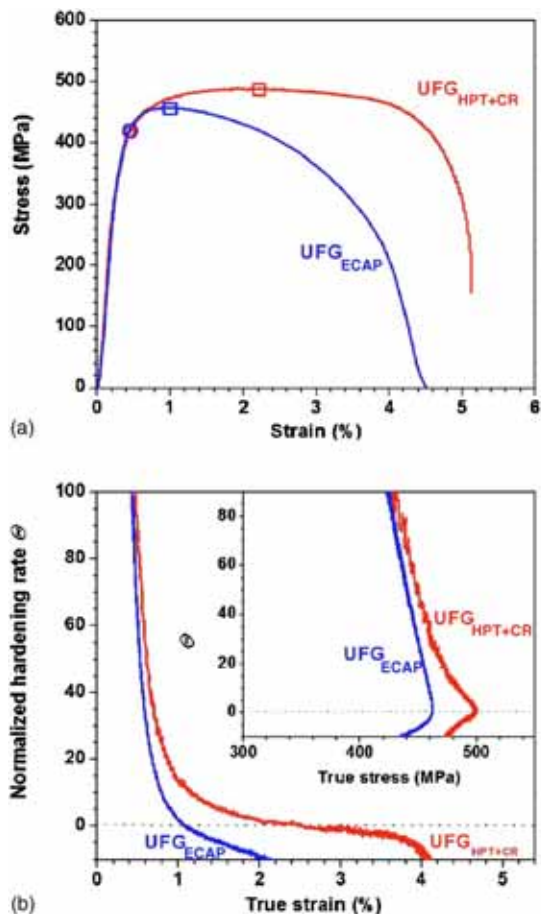


FIG. 1. (Color online) (a) Tensile engineering stress-strain curves of the UFG_{HPT+CR} and UFG_{ECAP} Cu samples: the open squares mark the uniform elongations and the open circles mark the 0.2% offset yield strengths. (b) Normalized strain-hardening rate Θ against the true strain. The inset shows curves of Θ against true stress.

creases to negative values after a small plastic strain. It is instructive to note also that these experiments used tensile samples with a thickness of 0.15 mm and work currently in progress suggests that thicker samples exhibit even higher ductilities due to a size effect.

TEM and EBSD investigations indicate that the UFG_{ECAP} sample contains a majority of LAGBs while the UFG_{HPT+CR} sample has a high fraction of HAGBs. As shown in Fig. 2(a), the majority of grain boundaries in the UFG_{ECAP} Cu are wavy and diffuse so that the difference in contrast between neighboring grains is slight. Both the slight contrast difference and the wavy and diffuse boundaries are caused by small orientation variations among the grains/subgrains which are primarily in a nonequilibrium state with extrinsic (nongeometrically necessary) dislocations or other interface defects.¹¹ By comparison, most of the grain boundaries in the UFG_{HPT+CR} sample are sharp and clear [Fig. 2(b)] and the contrast between neighboring grains is larger, thereby suggesting these are boundaries with higher misorientation angles. By tilting some grains to a $\langle 110 \rangle$ zone axis and checking the angle differences between neighboring grains/subgrains, it was concluded that the UFG_{HPT+CR} Cu contained a higher fraction of HAGB than the UFG_{ECAP} Cu. It appears that the HAGBs of the UFG_{HPT+CR} Cu were formed primarily during the HPT process,¹² together with partial re-

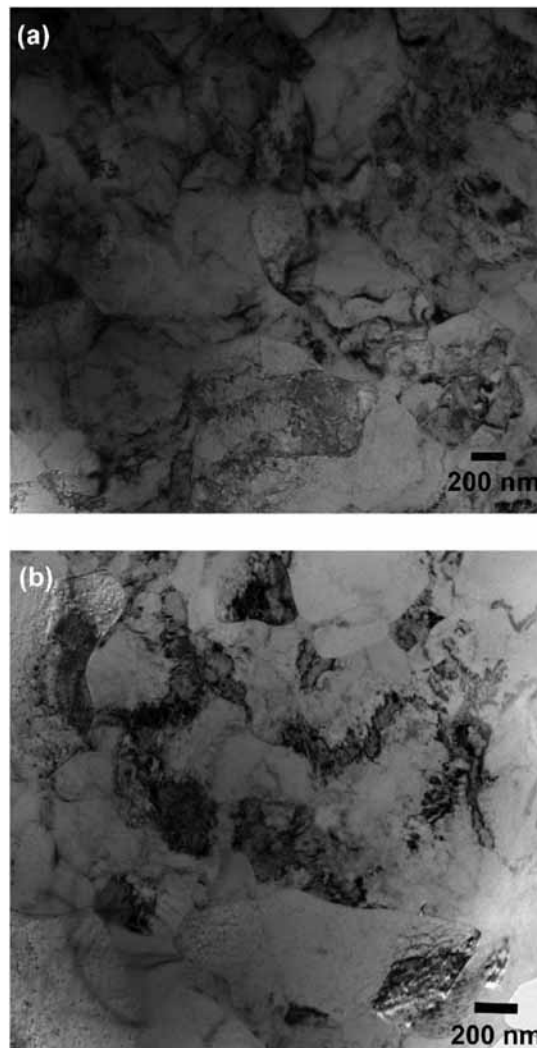


FIG. 2. Typical bright-field TEM images for the (a) UFG_{ECAP} Cu and (b) UFG_{HPT+CR} Cu samples. It is apparent that the grain boundaries in the UFG_{ECAP} sample are wavy and diffuse, while the grain boundaries in the UFG_{HPT+CR} sample are sharper and straighter than in the UFG_{ECAP} sample.

crystallization during CR as suggested by the EBSD observations. The average grain sizes measured from the TEM images are ~ 180 nm in UFG_{HPT+CR} Cu and ~ 290 nm in UFG_{ECAP} Cu.

The grain boundary misorientation distributions determined using EBSD are shown in Fig. 3. Considering all boundaries $>2^\circ$, the UFG_{HPT+CR} sample has $\sim 56\%$ of HAGBs with misorientations $>15^\circ$, whereas the UFG_{ECAP} sample has only $\sim 32\%$ of HAGBs. The various peaks observed in the UFG_{HPT+CR} misorientation distribution have three potential sources. First, a plane strain deformation texture developed during the rolling process and this yielded preferred misorientations at 35.3° , 35.6° , 43° , 45° , 46° , and 54.7° .¹³ Second, there may be preexisting $\Sigma 3$ (60°), $\Sigma 27a$ (31.6°), and $\Sigma 27b$ (35.4°) coincident-site lattice (CSL) boundaries that were inherited from the recrystallization twin population and associated boundary reaction networks within the initial microstructure.¹⁴ Third, CSL boundaries may develop from twin growth related to partial recrystallization of the UFG_{HPT+CR} microstructure during the rolling deformation. However, these peaks only account for $\sim 10\%$ of the

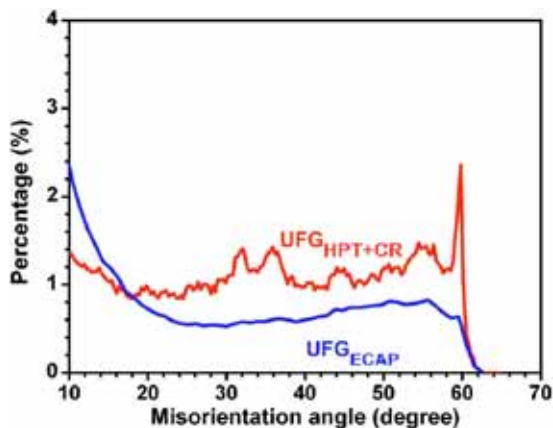


FIG. 3. (Color online) The distribution of grain boundary misorientation angles for the $\text{UFG}_{\text{HPT+CR}}$ and UFG_{ECAP} samples measured by EBSD with scanning step sizes of 70, 100, or 130 nm.

HAGBs in the $\text{UFG}_{\text{HPT+CR}}$ Cu sample. It follows therefore that the fraction of general HAGBs in the $\text{UFG}_{\text{HPT+CR}}$ Cu sample is $\sim 51\%$ and this is $\sim 20\%$ higher than in the UFG_{ECAP} sample where the fraction is only $\sim 32\%$.

The dislocation and twin densities of the $\text{UFG}_{\text{HPT+CR}}$ and UFG_{ECAP} Cu samples were analyzed by XRD.^{15,16} It was found that the dislocation density in $\text{UFG}_{\text{HPT+CR}}$ Cu was $\sim 2.3 \times 10^{14} \text{ m}^{-2}$, which is much smaller than that in UFG_{ECAP} Cu ($\sim 4.3 \times 10^{14} \text{ m}^{-2}$). This result was further confirmed by high-resolution TEM. The twin density, defined as the probability of finding a twin boundary between any two neighboring $\{111\}$ planes, was measured as $\sim 0.1\%$ for both the $\text{UFG}_{\text{HPT+CR}}$ and UFG_{ECAP} samples, respectively. Moreover, the XRD patterns showed that the UFG_{ECAP} has a $\{111\}$ texture and $\text{UFG}_{\text{HPT+CR}}$ has a $\{110\}$ rolling texture.

There is probably a simple explanation for the similar yield strengths of the $\text{UFG}_{\text{HPT+CR}}$ and UFG_{ECAP} samples. It is anticipated that the smaller grain size and larger fraction of HAGBs in the $\text{UFG}_{\text{HPT+CR}}$ Cu sample will increase the yield strength but this effect may be essentially cancelled by a decrease in strength due to the lower dislocation density. Moreover, this lower dislocation density provides additional confirmation that a recovery process was active during the SPD process in the $\text{UFG}_{\text{HPT+CR}}$ Cu sample.

These experimental results suggest that the presence of general HAGBs combined with a low dislocation density are more effective in enhancing the uniform elongation/toughness of UFG metals than LAGBs plus a high dislocation density. The mechanism for increasing strain hardening due to the presence of general HAGBs is not fully understood. One possibility is that HAGBs are more effective in blocking slipping dislocations, thereby forcing the dislocations to tangle and accumulate near the boundaries. By contrast, it is probably easier for slipping dislocations to react with extrinsic dislocations in the LAGBs and this may lead to an annihilation of dislocations and a near-zero dislocation accumulation as in the case of the UFG_{ECAP} Cu sample. Another possible mechanism for general HAGBs to increase the strain hardening is by the occurrence of grain boundary sliding since sliding has been observed experimentally in UFG

Al and Cu by SPD processing¹⁷ and it is well established that random HAGBs slide more easily than LAGBs.¹⁸ Furthermore, the presence of sliding will lead to dislocation emissions at triple junctions due to the presence of high stress concentrations and these dislocations may also act to increase the strain-hardening rate.

The lower dislocation density in the $\text{UFG}_{\text{HPT+CR}}$ sample is probably the main reason for its higher strain-hardening rate compared with the UFG_{ECAP} sample. The low dislocation density in $\text{UFG}_{\text{HPT+CR}}$ may allow further dislocation accumulation during the tensile tests, and this may lead to strain hardening. Earlier reports demonstrated that preexisting growth twins are effective in blocking and storing dislocations to give an improvement in strain-hardening rate.^{3,4} However, the influence of twin and other CSL boundaries in increasing the strain-hardening rate is essentially negligible in the present study because their fractions are small compared with the fraction of general HAGBs.

In summary, the present study demonstrates that a large fraction of equilibrium HAGBs and a low dislocation density can improve the toughness and uniform elongation of UFG materials. This study suggests an approach, based on imparting excessive processing plastic strain, by which the ductility of UFG materials may be improved. Furthermore, although the specimens used in the present study were relatively small, it should be noted that the same strategy may be easily scaled up for the processing of large bulk UFG materials for use in practical applications.

Y.H. Zhao, Y.Z. Zhou, and E.J. Lavernia would like to acknowledge support by the Office of Naval Research (Grant No. N00014-04-1-0370) with Dr. Lawrence Kabacoff as program officer.

- ¹C. C. Koch, D. G. Morris, K. Lu, and A. Inoue, *MRS Bull.* **24**, 54 (1999).
- ²Y. Wang, M. Chen, F. Zhou, and E. Ma, *Nature (London)* **419**, 912 (2002).
- ³Y. H. Zhao, J. F. Bingert, X. Z. Liao, B. Z. Cui, K. Han, A. Sergueeva, A. K. Mukherjee, R. Z. Valiev, T. G. Langdon, and Y. T. Zhu, *Adv. Mater. (Weinheim, Ger.)* **18**, 2949 (2006).
- ⁴Y. H. Zhao, Y. T. Zhu, X. Z. Liao, Z. Horita, and T. G. Langdon, *Appl. Phys. Lett.* **89**, 121906 (2006).
- ⁵Y. H. Zhao, X. Z. Liao, S. Cheng, E. Ma, and Y. T. Zhu, *Adv. Mater. (Weinheim, Ger.)* **18**, 2280 (2006).
- ⁶G. He, J. Eckert, W. Loeser, and L. Schultz, *Nat. Mater.* **2**, 3 (2003).
- ⁷K. X. Tao, H. Choo, H. Q. Li, B. Clausen, J. E. Jin, and Y. K. Lee, *Appl. Phys. Lett.* **90**, 101911 (2007).
- ⁸Y. M. Wang, E. Ma, R. Z. Valiev, and Y. T. Zhu, *Adv. Mater. (Weinheim, Ger.)* **16**, 328 (2004).
- ⁹R. Z. Valiev, I. V. Alexandrov, Y. T. Zhu, and T. C. Lowe, *J. Mater. Res.* **17**, 5 (2002).
- ¹⁰K. M. Youssef, R. O. Scattergood, K. L. Murty, J. A. Horton, and C. C. Koch, *Appl. Phys. Lett.* **87**, 091904 (2005).
- ¹¹J. Y. Huang, Y. T. Zhu, H. G. Jiang, and T. C. Lowe, *Acta Mater.* **49**, 1497 (2001).
- ¹²Y. H. Zhao, X. Z. Liao, Y. T. Zhu, Z. Horita, and T. G. Langdon, *Mater. Sci. Eng., A* **410-411**, 188 (2005).
- ¹³J.-H. Cho, A. D. Rollett, and K. H. Oh, *Metall. Mater. Trans. A* **35A**, 1075 (2004).
- ¹⁴V. Randle, B. Ralph, and D. Dingley, *Acta Metall.* **36**, 267 (1988).
- ¹⁵Y. H. Zhao, H. W. Sheng, and K. Lu, *Acta Mater.* **49**, 365 (2001).
- ¹⁶J. B. Cohen and C. N. J. Wagner, *J. Appl. Phys.* **33**, 2073 (1962).
- ¹⁷N. Q. Chinh, P. Szommer, Z. Horita, and T. G. Langdon, *Adv. Mater. (Weinheim, Ger.)* **18**, 34 (2006).
- ¹⁸M. Y. Gutkin, I. A. Ovid'ko, and N. V. Skiba, *J. Phys. D* **38**, 3921 (2005).